Quadrature-Induced Noise in Coriolis Vibratory Gyroscopes

Daryosh Vatanparvar and Andrei M. Shkel
MicroSystems Laboratory, Mechanical and Aerospace Engineering, University of California, Irvine, CA, USA
Email: {dvatanpa and andrei.shkel}@uci.edu

***Abstract*—In this paper, we present a model for noise performance estimation of Coriolis Vibratory Gyroscopes (CVG) in the presence of quadrature coupling. Analytical equations based on a low-order averaged model of a CVG were derived and used for numerical simulation of the Zero-Rate Output (ZRO) in the open-loop angular rate mode of operation. We demonstrated that as a result of the quadrature coupling and noise in the drive oscillation frequency, Quadrature Noise (QN) is introduced to the gyroscope output. For example, in the case of a Dual Foucault Pendulum (DFP) gyroscope with a frequency split on the order of 0.48 Hz, the QN was shown to have an experimentally measured Angle Random Walk (ARW) on the order of 0.39 ($deg/\sqrt{hr}$), which was orders of magnitude higher than a theoretical ARW of 0.0024 ($deg/\sqrt{hr}$) predicted by the Mechanical-Thermal Noise (MTN) model. This observed discrepancy was a motivation for the development of the model. A good agreement between the noise characteristics of the experimentally measured ZRO and a numerically simulated ZRO was observed, when accounting for the quadrature coupling. We concluded that the quadrature-induced noise is a major factor limiting the performance of high quality factor gyroscopes in nearly mode-matched conditions. This paper presents an analytical model for the noise estimation, which was supported experimentally.**

I. Introduction

Improvement of noise performance in miniaturized Coriolis Vibratory Gyroscopes (CVG) is an ongoing research topic. The topic includes identification of the fundamental noise sources and understanding the effects of fabrication imperfections and noise on performance limits in gyroscope operation. This understanding is essential for realization of Micro Electro-Mechanical (MEM) gyroscopes with navigational-grade and above navigational-grade performance.

Previously, analytical models have been reported for estimating the noise performance of CVGs operating in open-loop and closed-loop angular rate modes, [1-3]. In these models, the Zero-Rate Output (ZRO) noise estimation has been simplified down to modeling the motion along the sense axis with the mechanical-thermal noise acting as an input and the electronics pick-off noise acting on the gyroscope's output readout. However, due to fabrication imperfections, the quadrature coupling and coupling through anisotropic damping are inevitable, which not only result in a deterministic bias offset [4], but also contribute significantly to the noise in the ZRO.

Studies on the main sources of the ZRO in different gyroscope designs have been reported in [5,6]. While it is understood that the quadrature coupling results in loading of the pick-off electronics, limits the dynamic range, and affects the Bias Instability (BI) of a gyroscope, the noise introduced in the gyroscope output due to quadrature coupling has not been studied. In [6], it has been reported that a reduction in the gyroscope output voltage noise was observed after electrostatic tuning of the quadrature. This observation was hypothesized to be due to the phase uncertainty in the output signal.

This material is based on work supported by the Defense Advanced Research Projects Agency (DARPA) and U.S. Navy under Contract No. N66001-16-1-4021.

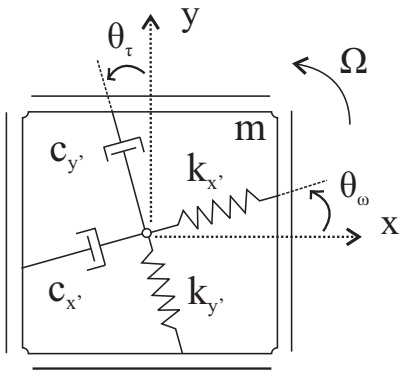

Fig. 1. A lumped-mass representation of a Coriolis vibratory gyroscope. Due to the mismatch of the principal axis of elasticity/damping, the noise in the drive mode is coupled to the sense mode channel and represents a major factor limiting the performance of nearly mode-matched vibratory gyroscopes.

In this paper, we demonstrate that due to the quadrature coupling, a stochastic error is introduced along the sense axis of a gyroscope. We derive equations based on an averaged gyroscope model to study the noise in the gyroscope output as a result of the quadrature coupling. Using the equations, we show that the output error has noise characteristics that are correlated to the noise characteristics of the oscillation along the drive axis. Experimental data of noise characterization using a Dual Foucault Pendulum (DFP) gyroscope [7] is presented and compared to predictions based on the quadrature noise model.

II. CVG Zero-rate Output

A single-axis CVG, in the most general form, consists of two mechanical vibration modes coupled through the Coriolis force. A common lumped-mass representation of a CVG is shown in Fig. 1. The equations of motion in an XY plane with axes aligned to the direction of electrostatic actuation and detection are

$$\begin{cases} m\ddot{x} + c_x\dot{x} + (c_{xy} - 2\alpha m\Omega)\dot{y} + k_x x + k_{xy} y = f_x, \\ m\ddot{y} + c_y\dot{y} + (c_{xy} + 2\alpha m\Omega)\dot{x} + k_y y + k_{xy} x = w_{BN}, \end{cases} \quad (1)$$

978-1-7281-2983-9/20/$31.00 ©2020 IEEE

where the state variables, x and y, represent the position of the shuttle along X and Y axes. Coefficients m, c_x, k_x, c_y, and k_y are the gyroscope's effective mass, damping and elasticity coefficients along the drive and sense axes, respectively. We denote the drive force, thermal noise, angular gain of the resonator and input rate with f_x, w_{BN}, α, and Ω, respectively.

In an ideal gyroscope, the motion along X and Y are coupled only through the Coriolis force. However, as shown in Fig. 1, due to fabrication imperfections a mismatch exists between the principal axes of elasticity, damping, and the actuation/detection axes. The mismatch angles in the principal axis of elasticity (θ_ω) and principal axis of damping (θ_τ) result in the elasticity and damping coupling terms represented using k_{xy} and c_{xy} coefficients, respectively. The elasticity and damping parameters in the equation of motion (1) are estimated using k'_x, c'_x, k'_y and c'_y coefficients through a coordinate transform as discussed in [4]. To simplify our analysis, we assume that the frequency mismatch is higher than damping mismatch, by several orders of magnitude. Therefore, we neglect the mismatch in the principal axis of damping ($\theta_\tau = 0$), i.e. the damping coupling c_{xy} is ignored.

In the zero-rate condition, the vibration amplitude along the sense axis, due to quadrature, is a function of the frequency split. In a case of operating a gyroscope with a frequency split higher than the bandwidth of the sense axis (on the order of 10 mHz), the vibration amplitude along the sense axis due to the quadrature coupling is orders of magnitude smaller that the vibration amplitude along the drive axis. Therefore, the quadrature force along the drive axis can be neglected (i.e. $k_{xy}.y \approx 0$).

Due to the assumption of a decoupled drive mode, the motion along the drive axis is studied using a one degree of freedom resonator model. In the drive mode, a Phase Locked Loop (PLL) controller is used to maintain the phase of vibration and tracks the corresponding changes in the resonant frequency. Additionally, a feedback force is implemented to control the amplitude of vibration along the drive axis. The vibration along the drive axis is represented as

$$x(t) = x_a(t)cos(\phi(t)) \tag{2}$$

In our analysis, the phase of vibration along the drive axis is used as a reference phase for signal modulation and demodulation.

As a result of the input and output noise in the oscillation circuit along the drive axis, the reference signal has additive noise both in the amplitude and frequency/phase of vibration. The noise in the reference signal is important since the quadrature force and the demodulation signal have the same noise characteristics. The drive amplitude of vibration and reference frequency are represented as

$$\begin{cases} x_a(t) = \bar{x}_a + x_N(t), \\ \dot{\phi}(t) = \bar{\omega} + \omega_N(t), \end{cases} \tag{3}$$

where $\bar{x}_a$ and $\bar{\omega}$ are the expected values of the drive amplitude and resonant frequency, which are equal to the set value of the PI controller and the resonant frequency along the drive axis ($\bar{\omega} = \omega_x = \sqrt{k_x/m}$), respectively. The ratio of the noise in the drive amplitude (x_N) to the expected value ($\bar{x}_a$) is on the order of 1ppm, [3]. Therefore, we conclude that the noise in the drive amplitude does not contribute to the noise along the sense axis at a frequency split higher than the bandwidth of the sense mode. However, the noise in the reference frequency (ω_N) results in phase errors in the gyroscope output affecting the gyroscope output noise. A model for frequency noise in oscillatory systems is discussed in [8].

In the case of vibration along the sense axis, the thermal noise, Coriolis coupling, and quadrature coupling act as input forces. The motion along the sense axis, demodulated using the reference signal, is in the form of

$$y(t) = y_c(t)cos(\phi(t)) + y_s(t)sin(\phi(t)) \tag{4}$$

where y_c and y_s are the in-phase and quadrature components of vibration along the sense axis, with reference to the vibration along the drive axis.

To estimate the ZRO, the first and second order time-derivatives of position ($\dot{y}, \ddot{y}$) were substituted in the equation of motion described in Eqn. (1). Due to orders of magnitude higher energy decay time in MEM gyroscopes, as compared to the time constant of vibration, the amplitude and frequency of vibration are considered to be slow-varying parameters. Therefore, the method of averaging can be applied [9] and the system is studied through the slow-varying parameters written in two equations as

$$\begin{cases} (\omega_y^2 - \dot{\phi_x}^2(t))y_s(t) - 2\dot{y_c}(t)\dot{\phi}(t) - y_c\ddot{\phi}(t) - 2\mu_y\dot{\phi}y_c(t) \\ -2\bar{x}_a\alpha\Omega\dot{\phi_x} = W_{BN1}(t)/\sqrt{2}, \\ (\omega_y^2 - \dot{\phi_x}^2(t))y_c(t) + 2\dot{y_s}(t)\dot{\phi}(t) + y_s\ddot{\phi}(t) + 2\mu_y\dot{\phi}y_s(t) \\ +\omega_{xy}^2\bar{x}_a = W_{BN2}(t)/\sqrt{2}, \end{cases} \tag{5}$$

where $\mu_y = c_y/(2m)$, $\omega_y = \sqrt{k_y/m}$, and $\omega_{xy}^2 = k_{xy}/m$. In Eqn. (5), the terms W_{BN1} and W_{BN2} represent the thermal noise, in units of force per system-mass (N/kg).

The components of the vibration amplitude along the sense axis, as described in Eqn. (4), are expressed as

$$\begin{cases} y_s(t) = \bar{y_s} + \epsilon_{ys}(t), \\ y_c(t) = \bar{y_c} + \epsilon_{yc}(t), \end{cases} \tag{6}$$

where $\bar{y_s}$ and $\bar{y_c}$ are the expected values of y_s and y_c. The terms $\epsilon_{ys}(t)$ and $\epsilon_{yc}(t)$ represent the noise in the demodulated output. The expected values of $y_s(t)$ and $y_c(t)$ are calculated by solving Eqn. (5), in absence of noise and in the steady-state condition. The expected values or deterministic bias offsets due to quadrature coupling are

$$\begin{cases} \bar{y_s} = \frac{-\omega_{xy}^2\bar{x}_a(2\mu_y\omega_x)}{(2\mu_y\omega_x)^2 + (\omega_y^2 - \omega_x^2)^2} \\ \bar{y_c} = \frac{-\omega_{xy}^2\bar{x}_a(\omega_y^2 - \omega_x^2)}{(2\mu_y\omega_x)^2 + (\omega_y^2 - \omega_x^2)^2} \end{cases} \tag{7}$$

In order to estimate the contribution of the quadrature coupling to the noise performance of the gyroscope, we use the averaged equation (5) to calculate the demodulated output

noise of the gyroscope (i.e., ϵ_{ys} and ϵ_{yc}). By substitution of Eqn. (3), (6) and (7) in Eqn. (5) and considering the noise terms up to the first order, an equation in the Laplace domain is derived and shown in Eqn. (8).

$$\begin{cases} \epsilon_{ys}(s)(\omega_y^2-\omega_x^2)+\epsilon_{yc}(s)(-2\omega_x s-2\mu_y\omega_x)=\frac{W_{BN1}(s)}{\sqrt{2}} \\ \qquad +\omega_N(s)(\bar{y_c}s+2\bar{y_s}\omega_x+2\mu_y\bar{y_c}) \\ \epsilon_{ys}(s)(2\omega_x s+2\mu_y\omega_x)+\epsilon_{yc}(s)(\omega_y^2-\omega_x^2)=\frac{W_{BN2}(s)}{\sqrt{2}} \\ \qquad +\omega_N(s)(-\bar{y_s}s+2\bar{y_c}\omega_x-2\mu_y\bar{y_s}) \end{cases} \tag{8}$$

The motion along the sense axis of the gyroscope is represented using two linear equations shown in Eqn. (8), with the mechanical-thermal noise and quadrature noise as input disturbances. In the presented model, we focus on understanding the noise output as a result of the quadrature coupling.

Using Eqn. (8), we derive a transfer function which correlates the gyroscope output noise (ϵ_{ys} and ϵ_{yc}) to the noise in the reference frequency (ω_N). The derived transfer function, shown in Eqn. (9), is used to numerically simulate the gyroscope output noise as a result of the quadrature coupling. Now, we can estimate the state variables (y_s) and (y_c) by combining the noise terms with the expected values, as described in Eqn. (6).

In practice, a phase delay in the demodulation process is used to decouple the rate and quadrature signal. This phase delay can be modeled using a rotation matrix acting on the demodulated output (with respect to the reference signal) as

$$\begin{bmatrix} y_{Quad} \\ y_{Rate} \end{bmatrix} = R(\phi') \begin{bmatrix} y_c \\ y_s \end{bmatrix} \tag{10}$$

One can show that the rotation matrix will have the form

$$R(\phi') = \frac{1}{\sqrt{(2\mu_y\omega_x)^2+(\omega_y^2-\omega_x^2)^2}} \begin{bmatrix} \omega_y^2-\omega_x^2 & 2\mu_y\omega_x \\ -2\mu_y\omega_x & \omega_y^2-\omega_x^2 \end{bmatrix} \tag{11}$$

By dividing the rate output by the scale factor, the ZRO output of the gyroscope, including the quadrature noise, can be modeled. The scale factor is estimated as

$$SF_M = \frac{1}{\sqrt{(\omega_y^2-\omega_x^2)^2+(2\mu_y\omega_x)^2}}.(2\bar{x}_a\alpha\omega_x) \tag{12}$$

Additionally, a white noise can be added to the rate and quadrature signal to model the noise due to pick-off electronics. In order to include the electronics noise, the state variables must be set in voltages, accounting for the pick-off gains. As discussed in the next section, the Power Spectrum Density (PSD) of the white noise in detection electronics is experimentally measured in (dB/Hz).

III. Experimental Results

A Dual Foucault Pendulum (DFP) gyroscope was used as the Device Under Test (DUT), [7]. The DFP has an operational frequency on the order of 15.03 kHz and a quality factor on the order of 1.1 M along both axes. The drive amplitude of the DFP ($\bar{x}_a$) was set to 268.9 mV, which is equivalent to a drive amplitude of 0.8 μm.

The noise performance of the DFP gyroscope was estimated by recording the gyroscope output for 8 hours and the results are shown in Allan Deviation (ADEV) and root-Power Spectrum Density (PSD) plots in Fig. 2. The experimental result illustrates an ARW of 0.39 $deg/\sqrt{hr}$ at a frequency split on the order of 0.48 Hz. While the ARW corresponding to electronics noise (estimated from PSD at frequencies well above the bandwidth of the gyroscope) was measured to be 0.17 $deg/\sqrt{hr}$.

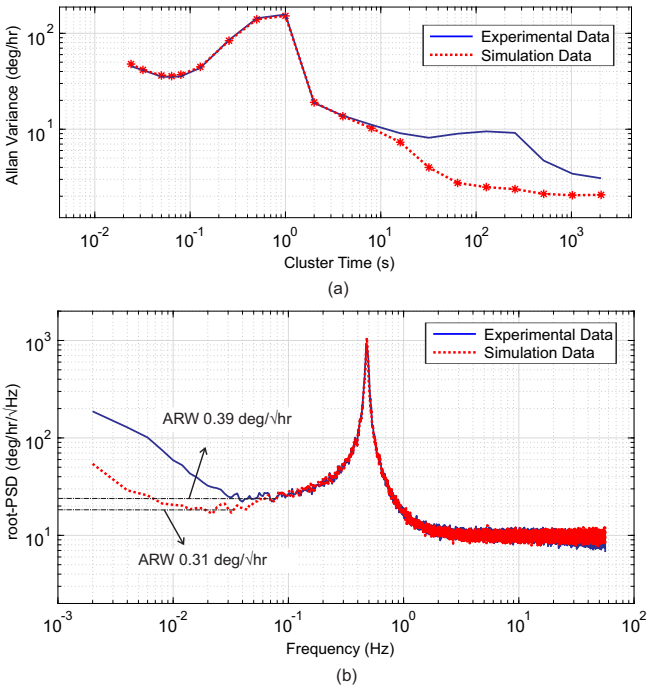

Fig. 2. A comparison of an experimentally measured and numerically simulated DFP's ZRO using ADEV and root-PSD plots. In (a), the Allan variance of the ZRO at different cluster times is shown. In (b), the Root-PSD plot of the ZRO is shown demonstrating an experimentally measured ARW and a predicted ARW of 0.39 and 0.31 $deg/\sqrt{hr}$, respectively.

The experimentally measured variations in the resonant frequency (ω_N), as an input disturbance, along with Eqn. (9) were used to estimate the state variables (y_s and y_c). Gyroscope parameters of the DFP are summarized in Table I and a PSD of -107.1 dB/Hz is estimated as the pick-off noise.

$$\begin{cases} \frac{\epsilon_{yc}(s)}{\omega_N(s)} = \frac{-(2s\omega_x+2\omega_x\mu_y)(\bar{y_c}s+2\bar{y_s}\omega_x+2\mu_y\bar{y_c})+(\omega_y^2-\omega_x^2)(-s\bar{y_s}+2\bar{y_c}\omega_x-2\mu_y\bar{y_s})}{(2s\omega_x+2\omega_x\mu_y)^2+(\omega_y^2-\omega_x^2)^2} \\ \frac{\epsilon_{ys}(s)}{\omega_N(s)} = \frac{(\omega_y^2-\omega_x^2)(\bar{y_c}s+2\bar{y_s}\omega_x+2\mu_y\bar{y_c})+(2s\omega_x+2\omega_x\mu_y)(-s\bar{y_s}+2\bar{y_c}\omega_x-2\mu_y\bar{y_s})}{(2s\omega_x+2\omega_x\mu_y)^2+(\omega_y^2-\omega_x^2)^2} \end{cases} \tag{9}$$

MATLAB's linear solver was used to numerically simulate the rate and quadrature output of the gyroscope. The noise characteristics were compared to the experimental data, shown in Fig. 2. A good agreement between the predicted output noise and measurements was observed. Since in our model, we did not consider the coupling due to anisotropic damping or the noise in the resonant frequency of the sense axis, the predicted ARW is 20% lower than the measured ARW, Fig. 2 (b).

TABLE I
EXPERIMENTALLY EXTRACTED GYROSCOPE PARAMETERS.

Parameters	**x**	**y**
Resonant Frequency (Hz)	15032	15031.52
Quality factor	1.15M	1.07M
Mass (kg)	5.96e-8	
Simulated Angular Gain	0.73	
Coupling Stiffness $(rad/s)^2$	4801.77	

The frequency split of the DFP can be reduced further down to below 20 mHz, which would improve the electronics noise ARW to a level of 0.004 $deg/\sqrt{hr}$. However, since the quadrature noise dominates at a low frequency split, the noise performance degrades as the frequency split is further reduced. The root-PSD of the characterized rate-output is shown in Fig. 3 for different frequency splits.

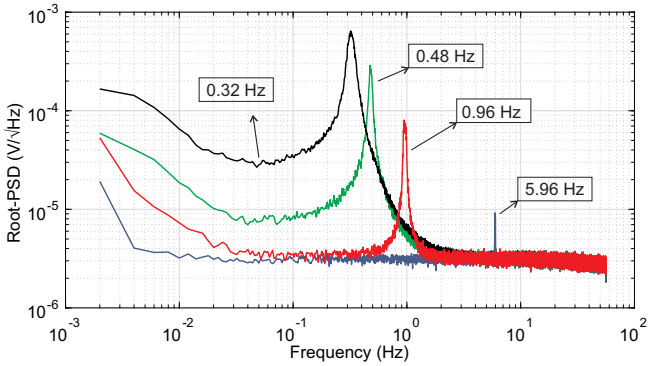

Fig. 3. Shown is the root-PSD plot of the DFP's rate output, for operation conditions with different frequency splits. An increase in the noise at frequencies below the bandwidth of the gyroscope is observed as the frequency split is reduced.

Estimation of the ARW limit due different noise sources, such as the electrical noise, the mechanical-thermal noise, and the quadrature noise was performed as a function of the frequency split, shown in Fig. 4. The results demonstrate that at frequency splits above 0.5 Hz the noise performance is limited by the electronics noise. However, at lower frequency splits, the noise performance is limited by the quadrature-induced noise. The prediction results show a good agreement with the experimentally measured ARWs.

IV. CONCLUSION

In this paper, we demonstrated that the quadrature coupling contributes to the noise output of a CVG. Analytical equations based on an averaged gyroscope model were derived for simulation of the zero-rate output of a gyroscope, including

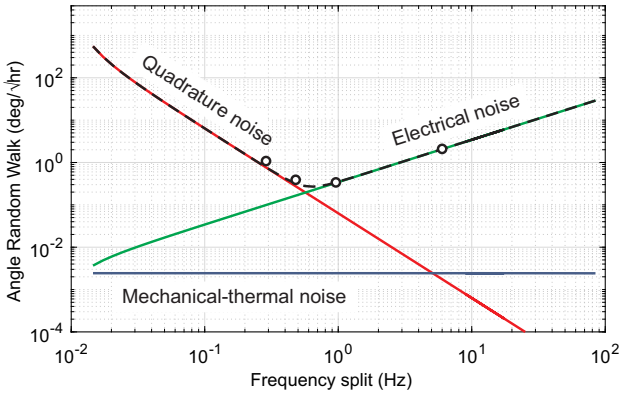

Fig. 4. Shown is the estimated ARW limit of the DFP gyroscope due to different noise sources including the mechanical-thermal noise, electrical noise and quadrature noise as a function of the frequency split. The circular points are experimental results showing a good agreement with the predicted trend in the total ARW as a function of the frequency split. This trade-off study is done for the DFP gyroscope under test with the characteristics reported in this paper.

the quadrature-induced noise. A good agreement between the experimental data and simulation result was observed. We concluded that at low frequency splits, due to the quadrature coupling and frequency noise in the drive mode oscillation, a noise is introduced to the gyroscope output. We demonstrated that while the pick-off noise is improved by electrostatic tuning of the frequency split, the quadrature noise is increased at low frequency splits, limiting the overall noise performance of the gyroscope. We concluded that to reach the fundamental mechanical-thermal noise limit of the DFP, which is on the order of 0.0024 $deg/\sqrt{hr}$, implementation of a quadrature-nulling control architecture along with mode-matching is essential.

REFERENCES

[1] D. Kim and and R.T M'Closkey, "Noise Analysis of Closed-Loop Vibratory Rate Gyros", American Control Conference (ACC), Montreal, QC, Canada, June, 2012.

[2] R. P. Leland, "Mechanical-thermal noise in MEMS gyroscopes," in IEEE Sensors Journal, vol. 5, no. 3, pp. 493-500, June 2005.

[3] D. Kim and R.T. M'Closkey, Dissecting Tuned MEMS Vibratory Gyros. In: Gorman J., Shapiro B. (eds) Feedback Control of MEMS to Atoms. Springer, New York, NY.

[4] D. Lynch, "Vibratory gyro analysis by the method of averaging", International Conference of Gyroscopic Technology and Navigation, St Petersburg, Russia, 1995.

[5] M. S. Weinberg and A. Kourepenis, "Error sources in in-plane silicon tuning-fork MEMS gyroscopes", in IEEE Journal of Microelectromechanical Systems, vol. 15, no. 3, pp. 479-491, June 2006.

[6] E. Tatar, S. E. Alper and T. Akin, "Quadrature-Error Compensation and Corresponding Effects on the Performance of Fully Decoupled MEMS Gyroscopes", in IEEE Journal of Microelectromechanical Systems, vol. 21, no. 3, pp. 656-667, June 2012.

[7] M. H. Asadian, S. Askari, I. B. Flader, Y. Chen, D. D. Gerrard, D. D. Shin, H. Kwon, T. W. Kenny and A. M. Shkel, "High Quality Factor Mode Ordered Dual Foucault Pendulum Gyroscope", IEEE Sensors Conference, New Delhi, India, Oct. 2018.

[8] P. Ward and A. Duwel, "Oscillator phase noise: Systematic construction of an analytical model encompassing nonlinearity." in IEEE Transactions on Ultrasonics, Ferroelectrics, and Frequency Control, vol. 58, no. 1, pp. 195-205, January 2011.

[9] J. B. Roberts and P. D. Spanos, "Stochastic averaging: An approximate method of solving random vibration problems", International Journal of Non-Linear Mechanics, vol. 21, no. 2, pp. 111-134, 1986.